Surface Structure and Morphology of Calcium Carbonate Polymorphs Calcite, Aragonite, and Vaterite: An Atomistic Approach

Nora H. de Leeuw* and Stephen C. Parker

School of Chemistry, University of Bath, Claverton Down, Bath BA2 7AY, UK

Received: October 2, 1997; In Final Form: February 4, 1998

Atomistic simulation techniques have been employed to investigate the effect of molecular adsorption of water on the low-index surfaces of calcite, aragonite, and vaterite. Calculated surface and hydration energies agree with experiment and previous calculations where available. Known experimental surface features are reproduced, i.e., 1×1 symmetry and structural features of the calcite $\{10\bar{1}4\}$ surface and bulk termination of the $\{10\bar{1}1\}$ and $\{11\bar{2}0\}$ surfaces. Surface carbonate groups tend to rotate to lie flat in the surface. The morphologies of the hydrated crystals agree with experimentally found morphologies. The bulk lattice energies of the polymorphs reflect their thermodynamic stability.

Introduction

Calcium carbonate is one of the most abundant minerals and important in many fields, including global CO_2 exchange, strong surface interactions with heavy metals in the environment,[1] scale formation and hence industrial water treatment,[2] energy storage,[3] and as a building block of shells and skeletons.[4] As such, the different polymorphs, but especially calcite, have been the subject of extensive and varied research, both experimentally and theoretically such as the LDA calculations of Skinner et al.[5] on bulk calcite showing mixed ionic and covalent bonding.

The surface structure of calcite has been studied by a variety of methods, both in ultrahigh vacuum, such as the SEM studies of the calcite $\{10\bar{1}4\}$and $\{10\bar{1}1\}$ surfaces,[6,7] and in air, such as the scanning force microscopy (SFM) study of step growth on the $\{10\bar{1}4\}$ plane.[8] AFM investigations under aqueous conditions[9] have been carried out to investigate a host of features such as distinct relaxation of surface oxygen ions on the $\{10\bar{1}4\}$ plane[10] and the role of steps and spiral dislocations in crystal growth.[11,12] Recent experimental and theoretical research has included the formation and growth of rhombohedral pits on the $\{10\bar{1}4\}$ surface.[13,14]

Apart from surface features of pure calcite, a growing area of research is growth inhibition and morphology change. As the concentration of calcium carbonate in many natural waters exceeds the saturation level, the precipitation of calcite in industrial boilers, transportation pipes, and desalination plants is of concern,[15] and it is therefore important to learn how morphology may be affected or induced. Often studies have concentrated on the incorporation in the crystal of foreign ions such as copper and manganese,[16] iron[17] and other divalent cations,[18−20] lithium,[21,22] phosphate species,[2,23] or organic matter.[24] Other methods of inducing morphology changes have included growing crystals using an organic template such as β-chitin[25] or an ammonium surfactant[24] to form aragonite, uncommon shapes of calcite,[27,28] or vaterite[29] displaying different faces depending on the template material used.[30,31]

Finally, Beruto and Giordani[4] have investigated the effect of induced electromagnetic fields to influence the morphology of calcium carbonate crystals.

The aim of the work described here is to investigate the effect of molecular adsorption, as opposed to dissociative adsorption, of water on the surface structure, energies, and hydration energies of the low index surfaces of calcite, aragonite, and their metastable polymorph vaterite. We found that all surfaces investigated would be hydrated to full monolayer coverage, and thus we concentrate on fully covered surfaces and compare different polymorphs of calcium carbonate with a view to obtain a better insight in the relative stabilities of the different structures.

Theoretical Methods

The surface geometry and energies of the calcium carbonates were modeled using atomistic simulation techniques. These are based on the Born model of solids[32] which assumes that the ions in the crystal interact via long-range electrostatic forces and short-range forces, including both the repulsions and the van der Waals attractions between neighboring electron charge clouds. The short-range forces are described by simple analytical functions that need to be tested using, for example, electronic structure calculations. The electronic polarizability of the ions is included via the shell model of Dick and Overhauser[33] in which each polarizable ion, in our case the oxygen ion, is represented by a core and a massless shell, connected by a spring. The polarizability of the model ion is then determined by the spring constant and the charges of the core and shell. These are usually obtained by fitting to experimental dielectric data when available.[34] When necessary, angle-dependent forces are included to allow directionality of bonding as, for instance, in the covalent carbonate anion.

We employed static simulations in this study to investigate the interactions between lattice ions and a full monolayer of water molecules to identify the strength of interaction with specific surface features. The static simulation code employed was METADISE,[35] which is designed to model dislocations, interfaces, and surfaces. Following the approach of Tasker,[36] the crystal consists of two blocks, each comprising two regions that are periodic in two dimensions. Region I contains those

* Corresponding author. tel 01225-826523; fax 01225-826231; e-mail n.h.deleeuw@bath.ac.uk.

S1089-5647(97)03210-0 CCC: $15.00
Published on Web 03/25/1998

atoms near the extended defect, in this case the surface layer and a few layers immediately below, and these atoms are allowed to relax to their mechanical equilibrium. Region II contains those atoms further away, which are kept fixed at their bulk equilibrium position and represent the rest of the crystal. The bulk of the crystal is simulated by the two blocks together while the surface is represented by a single block. Both regions I and II need to be sufficiently large for the energy to converge.

The surface energy is given by

$$\gamma = (U_s - U_b)/A \quad (1)$$

where U_s is the energy of the surface block of the crystal, U_b is the energy of an equal number of atoms of the bulk crystal, and A is the surface area. The energies of the blocks are essentially the sum of the energies of interaction between all atoms. The long-range Coulombic interactions are calculated using the Parry technique[37,38] whereas the short-range repulsions and van der Waals attraction are described by parametrized analytical expressions. The surface energy is a measure of the thermodynamic stability of the surface with a low, positive value indicating a stable surface.

In addition to providing a measure of the relative stabilities of the surfaces, the equilibrium morphology of a crystal is determined by the surface energy and the related growth rate of the various surfaces. Wulff's theorem[39] proposed that a polar plot of surface energy versus orientation of normal vectors would give the crystal morphology, while Gibbs[40] proposed that the equilibrium form of a crystal should possess minimal total surface free energy for a given volume. A surface with a high surface free energy has a large growth rate, and this fast growing surface will not be expressed in the equilibrium morphology of the resulting crystal. Only surfaces with low surface free energies and hence slow growing will be expressed. At 0 K, the surface free energy is a close approximation of the surface energy as calculated by static lattice simulations because the entropy term included in the surface free energy is small compared to the enthalpy term as the difference between the energies of the bulk and the surface is small. Thus, the surface energies can be assumed to determine the equilibrium morphology of the crystal.

A growth morphology is determined via a phenomenological approach using attachment energies.[41] These are defined as the energy per molecule released when one slice of thickness d_{hkl} crystallizes onto a crystal face (hkl). The relative growth rate of a face increases with increasing E_{att}, and similarly for the equilibrium morphology, the face with the highest value for E_{att} grows out while faces with low values of E_{att} are expressed in the growth morphology.

We used the potential parameters derived empirically by Pavese et al.[42] in their study of the thermal dependence of structural and elastic properties of calcite. The potential parameters used for the intra- and intermolecular interactions of the water molecule were obtained using the approach described in our previous study of water adsorption on MgO surfaces.[43] For the interactions between water molecules and calcium carbonate surfaces, we used the potential parameters previously fitted to calcite and described in a previous paper.[44] We verified these potential parameters by simulating the structure of ikaite, a calcium carbonate hexahydrate, and we found good agreement between calculated and experimental structural data. Calculating the change in enthalpy at 298 K for ikaite, calcite, and water, the change in interaction energy for the dissociation of ikaite per water molecule is 47 kJ mol^{-1}. This compares to experimental values of 47−50 kJ mol^{-1}.[45] In a previous paper[44] we used a reduced set of potential parameters for the intramolecular carbonate interactions, and in this case the interaction energy was found to be 30 kJ mol^{-1}. These present parameters are clearly in better agreement with the experimental findings. This means that we have a way of assessing the level of confidence in the potential model adequately describing the calcium carbonate polymorphs and their interactions with water and that the calculated heats of hydration will be a good indication of experimental energies.

TABLE 1: Surface, Attachment, and Hydration Energies of Calcite

surface (hexagonal indices)	γ_{pure}/ J m^{-2}	E_{attach} /kJ mol^{-1}	$\gamma_{hydrated}$/ J m^{-2}	$E_{hydration}$/ kJ mol^{-1}
$\{10\bar{1}4\}$	0.59	−75.4	0.16	−93.9
{0001}Ca	0.97	−334.3	0.68	−79.2
$\{000\bar{1}\}CO_3$	0.99	−204.7	0.38	−93.2
$\{10\bar{1}0\}$	0.97	−759.6	0.75	−100.5
$\{10\bar{1}1\}$Ca	1.23	−307.2	0.63	−113.4
$\{10\bar{1}1\}CO_3$	1.14	−276.7	0.81	−100.9
$\{11\bar{2}0\}$	1.39	−291.3	0.43	−138.5

Results

The hydration energy of molecular adsorption of water onto the calcium carbonate surfaces was calculated by comparing the energy of the pure surface and an isolated water molecule with the energy of the hydrated surface. For a selection of surfaces our study was extended to include hydration in a series of partial coverages in which case many possible configurations of the partially hydrated surfaces were investigated to make sure that the most stable configuration was located. The energies quoted in later sections refer to the energetically most favorable configuration obtained. In addition to the configurations of water molecules relative to each other on the surface, the water molecule itself can be adsorbed onto the surface in several different ways as well, e.g., coordinated by one hydrogen to a surface oxygen as is found experimentally at negatively charged clay surfaces,[46] bonded by its oxygen to a surface cation as is often found on uncharged clay surfaces,[47] or intermediate between these positions. Again, the energies quoted are for the most stable configuration of the most stable position.

Calcite. Calcite has a rhombohedral crystal structure with space group $R\bar{3}c$ and $a = b = 4.990$ Å, $c = 17.061$ Å, $\alpha = \beta = 90°$, and $\gamma = 120°$[48] and was calculated to be $a = b = 4.797$ Å, $c = 17.482$ Å, $\alpha = b = 90°$, and $\gamma = 120°$. We studied five surfaces, including the $\{10\bar{1}4\}$ surface which is found experimentally to be the dominant surface. The other surfaces considered are the {0001} basal plane and the $\{10\bar{1}0\}$, $\{10\bar{1}1\}$, and $\{11\bar{2}0\}$ surfaces. The {0001} and $\{10\bar{1}1\}$ surface can be terminated in two different ways, either by a layer of calcium ions or by carbonate molecules. We need to be confident that the most stable plane is considered, and therefore calculations have been performed on all possible planes for each surface. The surfaces were allowed to relax and their surface and attachment energies calculated (Table 1).

The $\{10\bar{1}4\}$ surface consists of layers containing both calcium ions and carbonate groups. The surface plane is always terminated with oxygen atoms. The layers contain two differently oriented carbonate groups, and as a result, the oxygen atoms on the surface are in two different but equivalent orientations. From the surface and attachment energies in Table 1, it is clear that the $\{10\bar{1}4\}$ surface is the most stable surface, both unhydrated and with adsorbed water, and as such it will be expressed in both the growth and equilibrium morphology of the crystal. This agrees with both previous calculations[22,23] and experimental findings.[2,4,12,49−52]

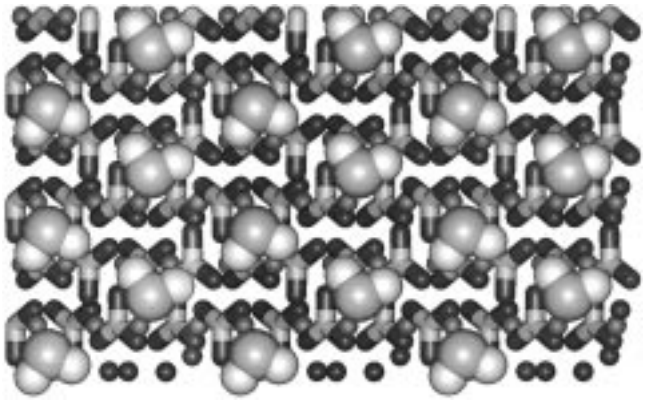

Figure 1. Top view of the hydrated calcite $\{10\bar{1}4\}$ surface, showing flat adsorption of water molecules in a regular pattern. The calcite framework is displayed as small balls for the Ca atoms and three-spoked wheels for the carbonate groups.

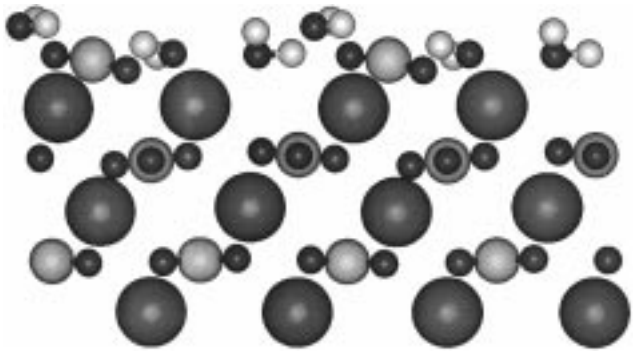

Figure 2. Hydrated carbonate terminated calcite {0001} surface showing clustering of the water molecules in the surface vacancies around the carbonate groups. The Ca atoms are displayed as large medium gray balls, the carbonate groups as three-spoked wheels with small dark balls for oxygen and medium sized balls for carbon, and the water molecules with small white balls for the hydrogen atoms.

The {0001} surface is a common twinning plane[48] and can be terminated by calcium atoms or carbonate groups. Both planes are dipolar, and this dipole needs to be removed.[53] Assuming stoichiometry, this is achieved by moving half the surface ions to the bottom of the unit cell, obtaining surfaces that are 50% vacant in either calcium ions or carbonate groups.[54] The two planes have the same surface energies although the attachment energies are very different, showing the carbonate plane to be the more favored surface. As the attachment energy of a plane is calculated for the unrelaxed surface, their trend can be compared to the surface energies of the unrelaxed surfaces. The surface energies of the unrelaxed planes are indeed very different (2.62 J m^{-2} for the Ca plane compared to 1.84 J m^{-2} for the carbonate plane), showing the unrelaxed carbonate plane to be more stable in agreement with the attachment energies. The difference between unrelaxed and relaxed surface energies indicates that substantial rearrangement and relaxation of the surface have taken place on energy minimization, due to the vacant sites on the surface. In fact, on the calcium terminated surface, the carbonate groups in the layer below rotate into the surface vacancies to form an edged surface with the surface calciums at the apex of the edges.

The dipolar $\{10\bar{1}0\}$ surface has the same surface energy of 0.97 J m^{-2}, again due to a large relaxation of the surface. The attachment energy is very large, indicating that this is a surface with a high growth rate.

The two $\{10\bar{1}1\}$ planes and the $\{11\bar{2}0\}$ surface all have fairly high surface energies and very similar attachment energies. Both the $\{10\bar{1}1\}$ and the $\{11\bar{2}0\}$ surface, which has only one nondipolar termination consisting of both calcium ions and carbonate groups, exhibit a bulklike termination.

Hydrated Surfaces. The water molecules adsorb uniformly onto the $\{10\bar{1}4\}$ surface in two orientations. Although initially positioned upright, after energy minimization their relaxed position is lying flat on the surface (Figure 1) which agrees with some configurations of water on clay surfaces.[55] The water molecules' oxygen atoms are coordinated to the surface calcium ions at a distance of 2.4 Å, with the two hydrogen atoms pointing toward two surface oxygen ions. On the fully hydrated surface, all surface oxygen atoms are coordinated to two hydrogen atoms from two different water molecules. Although the hydrogen-bond lengths are different for the two molecules (1.89 and 1.97 Å), the different orientations are still equivalent. The $\{10\bar{1}4\}$ surface exhibits 1×1 symmetry in accordance with the AFM images of the plane of calcite in water by Ohnesorge and Binnig.[9]

However, when the surface is only partially covered by water molecules, the difference between the two O- - -H bond lengths becomes important and the surface oxygens relax distinctly, showing a difference in height above the plane of about 0.05 Å. This effect has been observed by Liang et al.[12] in their AFM study of the $\{10\bar{1}4\}$ surface in water, who found that there was a structural difference between the oxygen ions of the differently orientated carbonate groups. They found an average difference in height with respect to the surface of approximately 0.35 Å, although they suggest that this is exacerbated by surface deformation due to the AFM tip. This variance in height was proposed[7,10] to be due to a different rotation of the carbonate groups in the carbonate planes. Our results agree with that proposition, although we cannot rule out a distinct distortion rather than rotation of the different carbonate groups. The fact that this result only occurs on partially hydrated surfaces is confirmed by Liang et al.,[10] who state that "water molecules are moved out of the way as the AFM tip scans the surface".

The hydrated calcium terminated {0001} plane shows a similar relaxation to the unhydrated plane. After energy minimization the surface has relaxed in the same way as the unhydrated surface, even though the starting position for the hydrated surface is an unrelaxed surface with adsorbed water molecules. The water molecules are adsorbed onto the calcium ions at the apex of the edges. It can be seen from Table 1 that although the Ca plane has been stabilized by hydration, it is to a much lesser extent than the $\{10\bar{1}4\}$ surface. The hydrated carbonate plane, however, has been stabilized by water adsorption to a much larger extent and is now the dominant of the two planes. In this case, the crystal surface has not relaxed appreciably, but the water molecules cluster around the surface carbonate groups filling in the vacant sites (Figure 2). The water molecules are not only coordinated to the surface, either with their oxygen atom to surface calcium ions or by hydrogen bonding to a surface oxygen, but also form extensive hydrogen bonding between themselves, with O- - -H distances ranging from 1.81 to 2.16 Å. The interactions between these adsorbed water molecules at full monolayer coverage account for an extra stabilizing energy factor of -1.5 kJ mol^{-1} compared to noninteracting water molecules.

On the $\{10\bar{1}0\}$ surface adsorption of water has not such a marked effect on the surface energy as with the {0001} surface although the hydration energy is considerable. The water molecules adsorb in rows in two alternating ways, either (i) coordinated by their oxygen atoms to a surface calcium ion and both hydrogens coordinated to surface oxygen ions and (ii) with

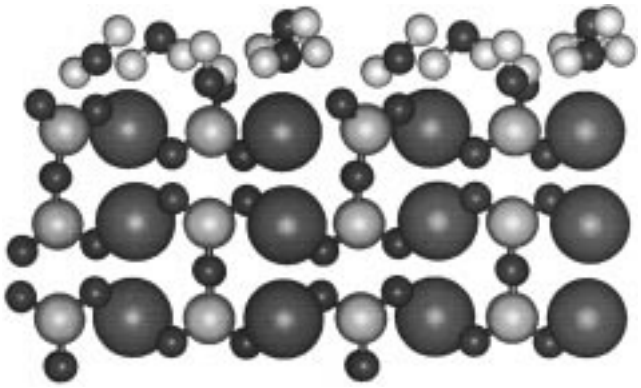

Figure 3. Hydrated calcite $\{11\bar{2}0\}$ surface showing bulk termination of the surface and different adsorption modes of the water molecules (Ca = large medium gray, C = medium sized pale gray, O = small dark gray, H = small white).

only one hydrogen coordinated to a surface oxygen. Although the water molecules do not interact with one another through proper hydrogen bonding (O- - -H distance is 2.4 Å), any other configuration is less energetically favorable.

In the hydrated crystal terminated by the $\{10\bar{1}1\}$ surface, only the surface carbonate groups rotate on relaxation, while the calcium ions and the carbonate groups from the third layer onward (ca. 6 Å) remain at their bulk positions. The water molecules adsorb in the vacancies resulting from the dipolar surface. They closely coordinate to both surface calcium and oxygen ions although no hydrogen bonding between the water molecules is evident. This relatively small rearrangement of the surface confirms the findings of Stipp and Hochella,[7] who studied the structure and bonding of the $\{10\bar{1}1\}$ cleavage plane by X-ray photoelectron sprectroscopy (XPS) and low-energy electron diffraction (LEED) to see whether hydration would lead to a thick, disordered or amorphous surface layer as suggested by Davids et al.[56] They found, however, that apart from some possible rotation of surface carbonate groups, the surface for at least 10 Å into the crystal was ordered with bulk lattice dimension, a result which our calculations have borne out.

Like the $\{10\bar{1}1\}$ surface, the hydrated $\{11\bar{2}0\}$ does not show any rearrangement of surface calcium or carbonate species (Figure 3). The plane is stabilized considerably by hydration with by far the largest hydration energy, and the water molecules adsorb in three distinct ways: (i) coordinated by its oxygen to three calcium ions at distances between 2.28 and 2.46 Å, (ii) coordinated by both hydrogens to surface oxygen ions at O- - -H distances of 1.53 and 1.56 Å, bridging two carbonate groups, and (iii) with only one hydrogen closely coordinated to a carbonate group. There is no appreciable hydrogen bonding between the adsorbed water molecules themselves and the very high hydration energy, and surface stabilization is thus entirely due to the close coordination of the water molecules to the surface.

Aragonite. Aragonite has an orthorhombic crystal structure with space group *Pmcn*. We started from the experimental structure found by Dickens and Bowen[57] with $a = 4.9598$ Å, $b = 7.9641$ Å, and $c = 5.7379$ Å and $\alpha = \beta = \gamma = 90°$. The bulk crystal was allowed to relax, giving $a = 4.8314$ Å, $b = 7.8359$ Å, $c = 5.7911$ Å, and $\alpha = \beta = \gamma = 90°$. The crystal was then cut to obtain the following low index surfaces: {010}, {100}, {001}, {110}, {011}, {101}, and {111}. The {010}, {011}, and {110} surfaces are generally expressed in the experimental morphology of the crystal.[58] The {010} and {110} surfaces are cleavage planes while the {110} is also a twinning plane. As with calcite all but one of the surfaces can be cut in more than one way, resulting in planes terminated by either calcium ions or oxygen atoms of the carbonate groups. The calculated surface and attachment energies are given in Table 2.

TABLE 2: Surface and Hydration Energies of Aragonite

surface	γ_{pure}/J m^{-2}	E_{attach}/ kJ mol^{-1}	$\gamma_{hydrated}$/ J m^{-2}	$E_{hydration}$/ kJ mol^{-1}
{010}Ca	0.96	−105.2	0.24	−105.2
{010}CO_3	1.50	−314.8	1.77	−21.2
{100}CO_3	1.50	−381.3	0.93	−122.6
{001}Ca	1.05	−341.1	0.62	−93.6
{001}CO_3	0.85	−120.1	0.90	−39.4
{110}Ca	0.88	−101.2	0.56	−94.6
{110}CO_3	1.04	−303.0	0.81	−80.8
{011}CO_3	0.69	−61.5	1.07	−8.2
{011}CO_3	1.16	−167.6	1.15	−45.4
{011}CO_3	0.99	−102.2	0.25	−113.8
{011}CO_3	1.13	−167.6	0.50	−133.7
{101}Ca	0.99	−145.6	0.53	−98.7
{101}CO_3	1.08	−155.5	0.62	−125.3
{111}Ca	1.40	−319.7	1.03	−118.5
{111}Ca	1.03	−257.3	0.79	−90.6
{111}CO_3	0.84	−177.1	0.64	−84.4
{111}CO_3	1.02	−257.3	0.72	−84.0

The surface energy of the pure {010} surface quoted in Table 2 shows the calcium terminated plane to have a lower surface energy than the carbonate surface and hence to be the more stable surface plane. The carbonate terminated plane shows considerable relaxation after energy minimization (cf. an unrelaxed surface energy of 3.58 and 1.50 J m^{-2} for the relaxed plane). The reason is that on relaxation the surface carbonate groups rotate to lie flat in the surface rather than upright as in a bulk termination. The calcium terminated plane on the other hand shows hardly any relaxation. The attachment energies agree with the surface energies in showing the calcium plane to be favored over the carbonate plane and with the experimental morphology through its low value indicating a small growth rate.

The {001} surface has a fairly low attachment energy approaching that of the calcium {010} plane, and as such we should expect to see it expressed in the growth morphology. Deer et al.[48] show some unresolved planes in their experimental morphology which from their angle and position may be the {001} surface which would agree with its low attachment energy.

In both the unhydrated and hydrated form the calcium terminated {110} surface is more stable than the carbonate plane. The calcium terminated surface does not relax appreciably on energy minimization, but the carbonate plane does, from an initial surface energy of 3.93 J m^{-2} to 1.04 J m^{-2} after relaxation. As with the {010} surface, this is due to the surface carbonate groups which rotate to lie flat. No such relaxation takes place on the calcium terminated plane, where the topmost carbonates are anchored by the surface calcium ions. The attachment energy of the carbonate plane is very high, reflecting the high surface energy of the unrelaxed surface.

The {011} surface has four different cuts which had to be investigated, all of which with one or more surface oxygen ions. However, their surface energies vary greatly as is shown in Table 2 from a very stable surface with $\gamma = 0.69$ J m^{-2} to the least stable which has a surface energy of 1.16 J m^{-2}. The attachment energies show the same trend as the relaxed surface energies with a very low value for the most stable plane, indicating that this surface would be expressed in the growth morphology.

Hydrated Surfaces. On hydration of the {010} surfaces the

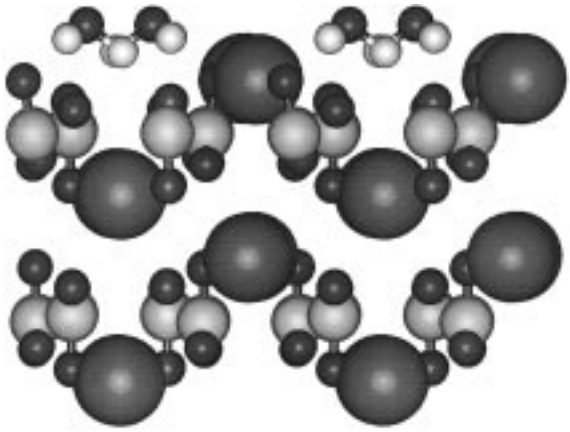

Figure 4. Hydrated calcium terminated aragonite {110} surface, showing bridgelike adsorption of the water molecules (Ca = large medium gray, C = medium sized pale gray, O = small dark gray, H = small white).

calcium terminated plane is stabilized by hydration as is shown in Table 2 by the decreased surface energy. In fact, this surface is the most stable of the hydrated surfaces with a very low surface energy of 0.24 J m^{-2}. The water molecules adsorb to the surface in two positions, although both are coordinated to a surface calcium as well as a surface oxygen through one of their hydrogens. There is some coordination between the two different water molecules, although 2.5 Å is too long a distance for a formal hydrogen bond.

In contrast, the carbonate terminated plane has been destabilized by hydration. Although the hydration energy shows that hydration is still energetically possible, the surface energy has increased, and it would thus be the very stable calcium terminated plane which is seen experimentally.

Similarly, the most stable of the four {011} planes is not further stabilized by hydration but shows instead a considerable increase in surface energy to 1.07 J m^{-2}. Its hydration energy at −8.2 kJ mol^{-1} is the least of the series and shows that adsorption of water onto this plane is only barely energetically favorable. Only two of the four planes show any stabilization due to hydration, both with very large hydration energies of −113.8 and −133.7 kJ mol^{-1}. One of these surfaces has become especially stable with a surface energy of 0.25 J m^{-2}. This is helped by the fact that the adsorbed water molecules not only closely coordinate to the surface ($Ca-O_{water}$ distances of 2.43−2.49 Å, $O_{lattice}-H$ distances of 1.48−1.63 Å) but also form an extensive network between themselves.

When viewing the hydrated calcium terminated plane of the {110} surface (Figure 4), it is clear that, apart from some small movement in the surface ions, notably a slight tilting of the carbonate groups, no comprehensive rearrangement of the surface layers has taken place. Although both surfaces are nondipolar, Figure 4 shows that the calcium plane appears to have surface vacancies due to the arrangement of the calcium ions in the bulk crystal. The water molecules, rather than adsorb above the surface calcium ions, prefer to adsorb with their hydrogen atoms coordinating to two surface oxygens bridging the apparent calcium vacancy between two carbonate groups. The distance between surface calcium and water oxygen ion is 2.53 Å, somewhat larger than average (ca. 2.4 Å), but the distances between surface oxygen and the water molecules' hydrogen atoms at 1.51 and 1.56 Å are very short for O- - -H bonding, and clearly the water molecules are closely coordinated to the surface. This is borne out by the hydration energy, which at −94.6 kJ mol^{-1}, while not the largest of the series of surfaces, is nevertheless appreciable.

TABLE 3: Surface and Hydration Energies of Vaterite

surface	γ_{pure}/J m^{-2}	E_{attach}/ kJ mol^{-1}	$\gamma_{hydrated}$/J m^{-2}	$E_{hydration}$/ kJ mol^{-1}
{010}Ca	1.35	−342.8	0.91	−91.7
{010}CO_3	0.62	−79.9	0.22	−86.8
{100}Ca	1.31	−168.6	0.69	−111.0
{100}CO_3	1.39	−137.1	0.55	−134.1
{001}Ca	1.40	−294.9	0.70	−85.9
{001}CO_3	1.58	−373.1	0.82	−111.9
{110}Ca	1.18	−249.9	0.52	−129.3
{110}CO_3	1.04	−149.1	0.63	−98.4
{011}Ca	1.22	−577.0	0.82	−100.3
{011}CO_3	0.93	−186.6	0.26	−106.7
{101}Ca	1.47	−186.2	0.35	−181.4
{101}CO_3	1.07	−176.2	0.68	−115.8
{111}Ca	0.82	−187.6	0.51	−88.8
{111}CO_3	0.85	−245.4	0.69	−78.1

All {100}, {101}, and {111} surfaces are stabilized by hydration as is the {001} calcium plane with hydration energies ranging from −90.6 to −125.3 kJ mol^{-1}. The hydrated {001} carbonate plane, on the other hand, has been destabilized although the hydration energy shows that water adsorption is still energetically favorable.

Vaterite. Vaterite, a metastable form of calcium carbonate and precursor of calcite and aragonite, is hexagonal with space group *P*63 and $a = b = 4.13$ Å, $c = 8.48$ Å, $\alpha = \beta = 90°$, and $\gamma = 120°$.[48] However, there is considerable disorder of the carbonate molecules leading to partial occupancies of different carbonate sites. For this reason we started from the experimental structure elucidated by Meyer[59] which uses space group *Pbnm* to describe the crystal without allowing for carbonate disorder. The unit cell is twice the size of the original cell, and the vectors and angles now become $a = 4.13$ Å, $b = 7.15$ Å, $c = 8.48$ Å, and $\alpha = \beta = \gamma = 90°$ which after energy minimization relaxed to $a = 4.43$ Å, $b = 6.62$ Å, $c = 8.04$ Å, and $\alpha = \beta = \gamma = 90°$. In this structure all surfaces have both calcium and carbonate terminated planes, and their surface and hydration energies are given in Table 3.

From Table 3 it is clear that the {010} carbonate plane is the dominant surface, both in the dry and as the hydrated form, with the lowest surface and attachment energies of the series. Although the calcium terminated plane is dipolar and hence is given vacancies in its surface, the carbonate plane is nondipolar and the pure surface does not relax appreciably (cf. unrelaxed surface energy of 0.78 J m^{-2} versus relaxed surface energy of 0.62 J m^{-2}).

The {100}, {001}, and {110} surfaces have relatively large surface and attachment energies, even though some surfaces have relaxed considerably. The dipolar {001} planes, for example, show extensive relaxation and rearrangement of the surface, especially the carbonate plane whose unrelaxed surface energy of 4.34 J m^{-2} drops to 1.58 J m^{-2}. On the calcium plane, the surface calcium ions relax into the second, carbonate, layer, some of which rotate their oxygen ions toward them. In the carbonate plane, the surface carbonate groups rotate to lie flat on the surface. The {011} calcium plane and both {101} surfaces are dipolar as well and again show extensive relaxation on energy minimization.

Hydrated Surfaces. Adsorption of water stabilizes all vaterite surfaces, especially the calcium {010} and {101} and carbonate {011} planes.

Unlike its unhydrated counterpart, the surface energy of the hydrated {010} carbonate surface does change considerably on energy minimization, from 3.15 to 0.22 J m^{-2}, but as Figure 5 shows, this is due to rotation of the water molecules rather than

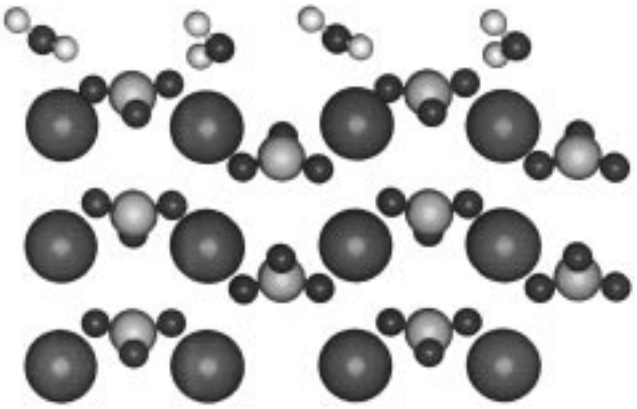

Figure 5. Hydrated carbonate terminated vaterite {010} surface, showing bulk termination of the carbonate groups and different adsorption modes of the water molecules (Ca = large medium gray, C = medium sized pale gray, O = small dark gray, H = small white).

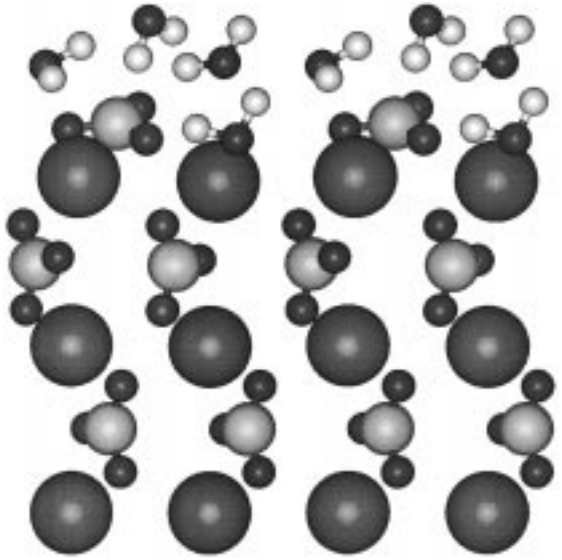

Figure 6. Hydrated carbonate terminated vaterite {001} surface, showing rotated surface carbonate groups and water molecules adsorbing in surface vacancies (Ca = large medium gray, C = medium sized pale gray, O = small dark gray, H = small white).

rearrangement of the surface lattice ions as in unhydrated surfaces. The water molecules adsorb in two distinct ways; both however are coordinated to a calcium ion and one lattice oxygen. The water molecules are too far apart for any hydrogen bonding to take place. The oxygen atoms of the water molecules appear to move into sites that would be occupied by lattice oxygens if another layer of material was lain down on the surface. This is similar to adsorption of water onto the MgO {310} surface, which we investigated in a previous paper[60] where we found that water molecules would adsorb with their oxygen on a lattice oxygen site and hydrogens pointing toward magnesium sites.

The high hydration energies of the {100}, {001}, and calcium {110} surfaces show that it is clearly energetically very favorable for water to adsorb onto these faces. On the hydrated {001} carbonate plane (Figure 6) some of the water molecules move into the carbonate vacancies created when removing the dipole. These are closely coordinated to a calcium ion and within H-bond distance of a lattice oxygen. The other water molecules that are adsorbed on top rather than in the surface are all coordinated to the surface oxygen ions by their hydrogen atoms. In addition to this coordination to the surface, there is an extensive network of hydrogen bonding between the adsorbed water molecules with O- - -H distances of ca. 1.8 Å.

On hydrating the dipolar calcium {101} plane, it becomes much more stable than the carbonate plane with a very low surface energy of 0.35 J m^{-2}, and at −181.4 kJ mol^{-1} the calcium plane also has the largest hydration energy of the series of vaterite surfaces. Like the carbonate {001} surface above the water molecules cluster in the calcium vacancies created when removing the dipole with one of the water molecules moving right into the surface coordinating to both a calcium and a carbonate oxygen in the second layer and another oxygen in the first carbonate layer. There is some coordination between the water molecules as two of the water molecules are within O- - -H distance of 2.1 Å. The same clustering occurs on the dipolar calcium {111} plane although there is no coordination between the different water molecules on this surface.

Discussion

Generally, the water molecules prefer to adsorb coordinated to calcium ions, although H bonding to the surface oxygen ions also takes place when possible. Even on surfaces that are greatly stabilized by water adsorption, the water molecules themselves often do not interact significantly which each other, indicating that adsorption to the surface outweighs possible intermolecular interactions between the water molecules, such as hydrogen bonding. These findings agree with calculations on hydrated MgO crystals.[43]

All calcite and vaterite surfaces are stabilized by the adsorption of a monolayer of water. The very low surface energy of the hydrated calcite $\{10\bar{1}4\}$ surface of 0.16 J m^{-2} agrees well with the experimental surface energy of the natural cleavage plane found by Gilman[61] of 0.23 J m^{-2}, particularly when taking into account that the experimental surface was mechanically cut and will contain steps and other dislocations which will increase the surface energy. The dominance of the $\{10\bar{1}4\}$ plane agrees with experimental work by, for example, Ohnesorge and Binnig[9] in their AFM study of calcite and by Heywood and Mann,[52] who showed optical micrographs of rhombohedral calcite crystals expressing the $\{10\bar{1}4\}$ surface under aqueous conditions. Furthermore, the hydration energies of calcite range from −79.2 to −138.5 kJ mol^{-1}, in good agreement with the binding energy quoted by Liang et al.[10] of −110.9 kJ mol^{-1} for water molecules adsorbed onto calcite, especially our hydration energy of −93.9 kJ mol^{-1} for the $\{10\bar{1}4\}$ surface.

Some of the aragonite surfaces, namely the carbonate {010} and, to a much lesser extent, the {001} plane, have been destabilized by the adsorption of water. The {010} carbonate plane is more unstable than the calcium terminated surface, in both the unhydrated and hydrated state. The unhydrated {001} carbonate plane, on the other hand, has a lower surface energy than its calcium counterpart, while on hydration the calcium plane becomes a lot more stable. The large stabilization of the calcium {010} surface confirms the suggestion of Aquilano and Rubbo,[62] who noted that the aragonite (010) surface was similar to that expressed by natural gypsum. They argued that the natural epitaxy of aragonite and gypsum implied that the (010) surface of aragonite must fit well on the water double layer of (010) gypsum, from which they implied that water on the aragonite (010) surface adsorbs in a quasi-ordered layer and stabilizes this surface.

Morphology. Wulff[39] and Gibbs[40] showed that equilibrium morphologies can be obtained from the surface energies (Tables 1−3). In contrast, a growth morphology is obtained from the attachment energies.[41] This is a simple, but successful, phenomenological model which relates the attachment energies to the rate of growth. The morphologies of calcite are shown in

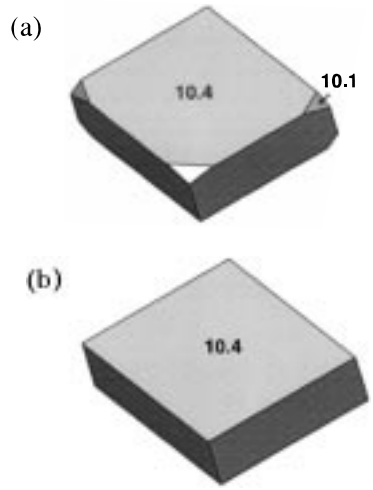

Figure 7. (a) Equilibrium morphology of unhydrated calcite and (b) growth morphology and equilibrium morphology of hydrated calcite crystal.

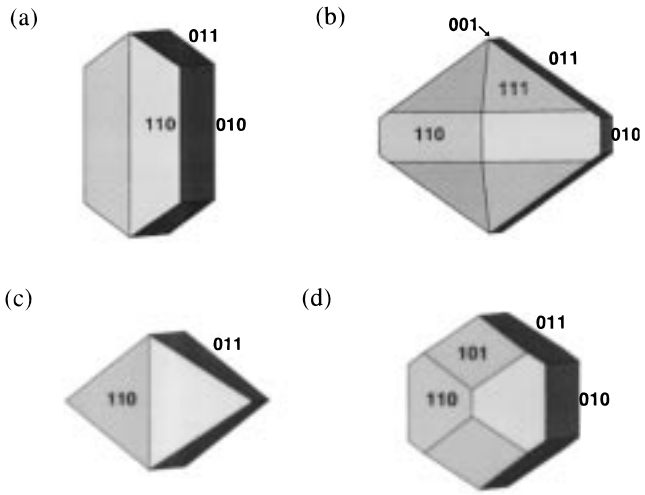

Figure 8. (a) Experimental morphology of aragonite, (b) equilibrium and (c) growth morphology of unhydrated aragonite, and (d) equilibrium morphology of hydrated aragonite crystal.

Figure 7. The equilibrium morphology of the unhydrated crystal shows a residual $\{10\bar{1}1\}$ face, the effect of relaxation which disappears on hydration, in agreement with the experimental morphology where only the dominant $\{10\bar{1}4\}$ face is expressed.[28,51]

In aragonite the equilibrium morphology of the hydrated aragonite crystal (Figure 8d) resembles the experimental morphology (Figure 8a) more closely than the unhydrated form (Figure 8b), which expresses the {111} which is not found experimentally.[58] There is also some residual {001} face in the unhydrated morphology which is sometimes found experimentally.[48] The calculated hydrated morphology agrees very well with the experimental morphology, being elongated and expressing the {010}, {011}, and the {110} faces,[58] although the {101} surface is too stable. Heywood and Mann[52] found that the predominant morphological form of aragonite expresses the {110} faces. The growth morphology (Figure 8c) shows the {011} and {110} faces in agreement with experiment[48] but not the {010} plane.

Less is known about the experimental morphology of vaterite under neutral conditions, other than that it can be found as spheres comprising needlelike units[15] or ellipsoidal[63] and disklike[51] crystals. The unhydrated equilibrium morphology (Figure 9a) does not resemble either needles or disks although

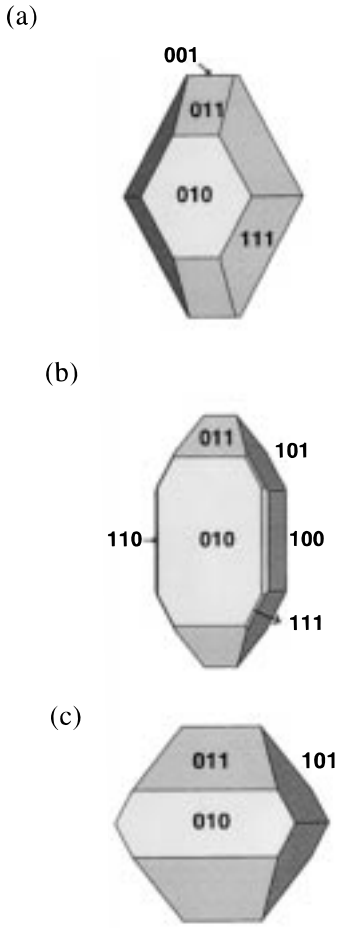

Figure 9. (a) Equilibrium morphology of unhydrated vaterite, (b) growth morphology, and (c) equilibrium morphology of hydrated vaterite crystal.

TABLE 4: Calculated Lattice Energies of Calcite, Aragonite, and Vaterite

polymorph	bulk lattice energy/10^8 kJ m^{-3}
calcite	−1.6867
aragonite	−1.7851
vaterite	−1.6577

it is somewhat ellipsoidal, as is the growth morphology (Figure 9b). The hydrated equilibrium morphology (Figure 9c) is more disklike in line with observed morphology.

According to Gibbs,[40] the energy of a crystal is made up of two components: a surface component, which is important when the crystals are small, and a bulk component, which becomes dominant at larger volumes:

$$E = \sum_i \gamma_i A_i + E_{\text{lattice}}$$

The bulk lattice energies of calcite, aragonite, and vaterite are given in Table 4. It is clear that at large volumes, when the surface component has become insignificant, aragonite will be the most stable form of calcium carbonate. These calculations have ignored temperature and zero-point energy, and the surface energies do not take into account entropy. Previous work[36] has shown that these are not critical approximations, and our findings agree with experiment; i.e., calcite is only more stable than aragonite because of its higher entropy.[4,64]

The surface component at any given volume for the three polymorphs is always positive and for the hydrated surfaces

can be expressed as a ratio calcite:aragonite:vaterite of 1.0:2.0:1.6. Thus, when the crystals are small enough for the bulk lattice energy to be insignificant, calcite is more stable than either aragonite or vaterite, although vaterite will be more stable than aragonite. This confirms that when vaterite is observed in calcium carbonate precipitation,[3] this is due to kinetic rather than thermodynamic factors.

Conclusion

We have employed atomistic simulation techniques to investigate the effect of hydration on the surface structure and stability of the low-index planes of calcite, aragonite, and vaterite. As a result, we can make the following observations:

When surfaces with two or more possible cuts are terminated by carbonate planes, the surfaces where the carbonate groups are lying flat will usually show bulk terminations, but the surfaces where the carbonate groups are upright will display rotation of these groups to lie flat in the surface.

The surface and hydration energies for calcite are in excellent agreement with experimental findings[61] and previous calculations[10] giving confidence that they are also accurate for aragonite and vaterite.

The $\{10\bar{1}4\}$ surface is the most stable surface of calcite. Hydration of the surfaces has a stabilizing effect, and the growth and hydrated equilibrium morphology of the crystal agree with the experimentally found morphology.

The $\{10\bar{1}4\}$ surface exhibits the same 1×1 symmetry and structural features of the surface oxygen ions as is found experimentally.[9,10] Our calculations showed a distinct relaxation or rotation of differently oriented but otherwise equivalent surface carbonate groups when the surface is partially hydrated.

In agreement with LEED experiments,[7] the $\{10\bar{1}1\}$ surface and also the $\{11\bar{2}0\}$ plane both exhibit bulklike termination of the surface with only some rotation of surface carbonate groups.

The calculated equilibrium morphology of the hydrated aragonite closely resembles its experimental morphology.[48]

The stability and regularity of the hydrated {010} surface of aragonite confirms the theory of Aquilano and Rubbo[62] based on natural epitaxy of the aragonite (010) and gypsum (010) surfaces stating that the aragonite (010) surface should be stabilized by an ordered water layer to be able to fit well onto hydrated gypsum (010).

The calculated equilibrium morphology of the hydrated vaterite crystals resembles disks in agreement with vaterite crystals found by Didymus et al.[51] The unhydrated and growth morphologies are elongated and perhaps more needlelike.[15]

The bulk lattice energies of the three polymorphs reflect their thermodynamic stability, in that the stability of calcite over aragonite is due to its higher entropy content at elevated temperatures rather than its bulk lattice energy, which favors aragonite.

The relative surface contributions of the polymorphs show that in the crystal nucleation stage calcite is the most stable form while aragonite becomes more stable when the crystal is large enough for the bulk lattice energy to outweigh the surface energy terms.

The results presented above show that atomistic simulation techniques are a viable tool for modeling the bonding of molecules to the surfaces of inorganic crystals. In the future, we aim to extend our study to include dynamics to model the effect of temperature on the solid properties and the dynamics of interactions between water and calcium carbonate surfaces.

Acknowledgment. We thank EPSRC for financial support. We wish to acknowledge the use of the EPSRC's Chemical Database Service at Daresbury.

References and Notes

(1) Park, N.-S.; Kim, M.-W.; Langford, S. C.; Dickinson, J. T. *J. Appl. Phys.* **1996**, *80*, 2680.
(2) Dove, P. M.; Hochella, M. F. *Geochim. Cosmochim. Acta* **1993**, *57*, 705.
(3) Chakraborty, D.; Bhatia, S. K. *Ind. Eng. Chem. Res.* **1996**, *35*, 1995.
(4) Beruto, D.; Giordani, M. *J. Chem. Soc., Faraday Trans.* **1993**, *89*, 2457.
(5) Skinner, A. J.; La Femina, J. P.; Jansen, H. J. F. *Am. Mineral.* **1994**, *79*, 205.
(6) Goni, S.; Sobrado, L.; Hernandez, M. S. *Solid State Ionics* **1993**, *63*, 786.
(7) Stipp, S. L.; Hochella, M. F. *Geochim. Cosmochim. Acta* **1991**, *55*, 1723.
(8) Stipp, S. L.; Gutmannsbauer, W.; Lehmann, T. *Am. Mineral.* **1996**, *81*, 1.
(9) Ohnesorge, F.; Binnig, G. *Science* **1993**, *260*, 1451.
(10) Liang, Y.; Lea, A. S.; Baer, D. R.; Engelhard, M. H. *Surf. Sci.* **1996**, *351*, 172.
(11) Gratz, A. J.; Hillner, P. E.; Hansma, P. K. *Geochim. Cosmochim. Acta* **1993**, *57*, 491.
(12) Hillner, P. E.; Manne, S.; Hansma, P. K. *Faraday Discuss.* **1993**, *95*, 191.
(13) Liang, Y.; Baer, D. R.; McCoy, J. M.; Amonette, J. E.; LaFemina, J. P. *Geochim. Cosmochim. Acta* **1996**, *60*, 4883.
(14) McCoy, J. M.; LaFemina, J. P. *Surf. Sci.* **1997**, *373*, 288.
(15) Chakraborty, D.; Agarwal, V. K.; Bhatia, S. K.; Bellare J. *Ind. Eng. Chem. Res.* **1994**, *33*, 2187.
(16) Nassralla-Aboukais, N.; Boughriet, A.; Fischer, J. C.; Wartel, M.; Langelin, H. R.; Aboukais, A. *J. Chem. Soc., Faraday Trans.* **1996**, *92*, 3211.
(17) Katz, J. L.; Reick, M. R.; Herzog, R. E.; Parsiegla, K. I. *Langmuir* **1993**, *9*, 1423.
(18) Compton, R. G.; Brown, C. A. *J. Colloid Interface Sci.* **1994**, *165*, 445.
(19) Brecevic, L.; Nothig-Laslo, V.; Kralj, D.; Popovic, S. *J. Chem. Soc., Faraday Trans.* **1996**, *92*, 1017.
(20) Deleuze, M.; Brantley, S. L. *Geochim. Cosmochim. Acta* **1997**, *61*, 1475.
(21) Rajam, S.; Mann, S. *J. Chem. Soc., Chem. Commun.* **1990**, 1789.
(22) Parker, S. C.; Kelsey, E. T.; Oliver, P. M.; Titiloye, J. O. *Faraday Discuss.* **1993**, *94*, 75.
(23) Kenway, P. R.; Oliver, P. M.; Parker, S. C.; Sayle, D. C.; Sayle, T. X. T.; Titiloye, J. O. *Mol. Simul.* **1992**, *9*, 83.
(24) Cicerone, D. S.; Regazzoni, A. E.; Blesa, M. A. *J. Colloid Interface Sci.* **1992**, *154*, 423.
(25) Falini, G.; Albeck, S.; Weiner, S.; Addadi, L. *Science* **1996**, *271*, 67.
(26) Walsh, D.; Mann, S. *Nature* **1995**, *377*, 320.
(27) Wong, K. K. W.; Brisdon, B. J.; Heywood, B. R.; Hodson, A. G. W.; Mann, S. *J. Mater. Chem.* **1994**, *4*, 1387.
(28) Archibald, D. D.; Qadri, S. B.; Gaber, B. P. *Langmuir* **1996**, *12*, 538.
(29) Litvin, A. L.; Samuelson, L. A.; Charych, D. H.; Spevak, W.; Kaplan, D. L. *J. Phys. Chem.* **1995**, *99*, 12065.
(30) Mann, S.; Heywood, B. R.; Rajam, S.; Birchall. J. D. *Nature* **1988**, *334*, 692.
(31) Didymus, J. M.; Mann, S.; Benton, W. J.; Collins, I. R. *Langmuir* **1995**, *11*, 3130.
(32) Born, M.; Huang, K. *Dynamical Theory of Crystal Lattices*; Oxford University Press: Oxford, 1954.
(33) Dick, B. G.; Overhauser, A. W. *Phys. Rev.* **1958**, *112*, 90.
(34) Colbourn, E. A. *Surf. Sci.* **1992**, *15*, 281.
(35) Watson, G. W.; Kelsey, E. T.; de Leeuw, N. H.; Harris, D. J.; Parker, S. C. *J. Chem. Soc., Faraday Trans.* **1996**, *92*, 433.
(36) Tasker, P. W. *Philos. Mag.* **1979**, *39*, 119.
(37) Parry, D. E. *Surf. Sci.* **1975**, *49*, 433.
(38) Parry, D. E. *Surf. Sci.* **1976**, *54*, 195.
(39) Wulff, G. *Z. Kristallogr. Kristallgeom.* **1901**, *34*, 949.
(40) Gibbs, J. W. *Collected Works;* Longman: New York, 1928.
(41) Hartman, P.; Bennema, P. *J. Cryst. Growth* **1980**, *49*, 145.
(42) Pavese, A.; Catti, M.; Parker, S. C.; Wall, A. *Phys. Chem. Miner.* **1996**, *23*, 89.
(43) de Leeuw, N. H.; Watson, G. W.; Parker, S. C. *J. Chem. Soc., Faraday Trans.* **1996**, *92*, 2081.
(44) de Leeuw, N. H.; Parker, S. C. *J. Chem. Soc., Faraday Trans.* **1997**, *93*, 467.

(45) Bischoff, J. L.; Fitzpatrick, J. A.; Rosenbauer, R. J. *J. Geol.* **1993**, *101*, 21.
(46) Delville, A.; Letellier, M. *Langmuir* **1995**, *11*, 1361.
(47) Bridgeman, C. H.; Skipper, N. T. *J. Phys.: Condens. Matter* **1997**, *9*, 4081.
(48) Deer, W. A.; Howie, R. A.; Zussman, J. *Introduction to the Rock Forming Minerals*; Longman: Harlow, UK, 1992**.**
(49) Blanchard, D. L.; Baer, D. R. *Surf. Sci.* **1992**, *276*, 27.
(50) MacInnes, I. N.; Brantley, S. L. *Geochim. Cosmochim. Acta* **1992**, *56*, 1113.
(51) Didymus, J. M.; Oliver, P. M.; Mann, S.; De Vries, A. L.; Hauschka, P. V.; Westbroek, P. *J. Chem. Soc., Faraday Trans.* **1993**, *89*, 2891.
(52) Heywood, B. R.; Mann, S. *Chem. Mater.* **1994**, *6*, 311.
(53) Tasker, P. W. *J. Phys. C: Solid State Phys.* **1979**, *12*, 4977.
(54) Oliver, P. M.; Parker, S. C.; Mackrodt, W. C. *Model. Simul. Mater. Sci. Eng.* **1993**, *1*, 755.
(55) Chang, F.-R. C.; Skipper, N. G.; Sposito, G. *Langmuir* **1995**, *11*, 2734.
(56) Davids, J. A.; Fuller, C. C.; Cook, A. D. *Geochim. Cosmochim. Acta* **1987**, *51*, 1477.
(57) Dickens, B.; Bowen, J. S. *J. Res. Natl. Bur. Stand., Sect. A: Phys. Chem.* **1971**, *75*, 27.
(58) Dana, E. S. *A Textbook of Mineralogy*; John Wiley & Sons: New York, 1958.
(59) Meyer, H. J. *Fortsch. Mineral.* **1960**, *38*, 186.
(60) de Leeuw, N. H.; Watson, G. W.; Parker, S. C. *J. Phys. Chem.* **1995**, *99*, 17219.
(61) Gilman, J. J. *J. Appl. Phys.* **1960**, *31*, 2208.
(62) Aquilano, D.; Rubbo, M. *Mater. Sci. Forum* **1996**, *203*, 193.
(63) Kabasci, S.; Althaus, W.; Weinspach, P.-M. *Trans. Inst. Chem. Eng. A* **1996**, *74*, 765.
(64) Tauson, V. L.; Abramovich, M. G.; Akimov, V. V.; Scherbakov, V. *Geochim. Cosmochim. Acta* **1993**, *57*, 815.